CHAPTER 5

DESIGN AND PERFORMANCE IMPROVEMENT STUDIES OF W-BAND GYRO-TWYSTRON USING CLUSTERED CAVITY

5.7. Introduction

5.8. Analysis and Design of Interaction Circuit

5.9. Modeling and Cold Simulation

5.10. PIC Simulation Results

5.11. Parametric Analysis and Validation

5.12. Conclusion

5.1. Introduction

The gyro-twystron is a hybrid device composed of the input cavity of gyro-klystron and the output waveguide section of the gyro-TWT. This hybrid amplifier's structure allows it to resolve the breakdown issue of the gyro-klystron and is less vulnerable to spurious oscillation than the gyro-TWT. Adding different cavities and drift tube sections between the input and output segments improves the device gain and the bandwidth and make it a valuable candidate for millimeter wave radar applications (i.e., space debris detection, weather monitoring, asteroid tracking) [26],[34]

Gyro-amplifiers are envisaged to find significant radar applications, especially in the Ka-band (26.5-40 GHz) and W-band millimeter-wave bands (75–110 GHz). Radars typically use atmospheric windows at 35 GHz and 94 GHz in these bands. The gyro-amplifiers required for radar applications must usually be capable of high average power and bandwidth. This urge for wide bandwidth led to exploring various methods to improve the device output performance. Thus, considerable research is being conducted on developing various approaches for increasing the device's bandwidth. There are two basic strategies used for bandwidth enhancement. The first way is stagger tuning, which effectively broadens the bandwidth by detuning cavities resonance frequency [116]. The stagger tuning technique is commonly used in cavity-based gyro amplifiers to increase bandwidth at the expense of gain decrement. As a result, a choice between gain and bandwidth must be made, even though stagger tuning can only extend the bandwidth to a certain level. The effect of stagger tuning on the various design of GKL was carried out University of Maryland and Naval Research Laboratory (NRL) [171]. At NRL Blank *et. al.* designed a stagger tuned multi-cavity gyro klystron for millimeter wave radar system and reported 80 kW output power with the bandwidth of 740 GHz [124]. Nusinovich and Chen et al. have explored the linear and nonlinear

theories associated with staggered tuned gyro-twystron, and have observed a substantial improvement in bandwidth and gain-bandwidth product in contrast to synchronous tuning [119], [120]. The effect of the stagger tuning on the performance of the multi-cavity based conventional gyro-twystron has been explored in [169].

Another concept for enlarging the bandwidth of the device has been proposed by R. Symons [117] for the conventional klystron study. This concept is based on clustered cavities and is employed to determine the complication of narrow bandwidth associated with cavity-related gyro amplifiers with minimum degradation of gain and efficiency. In this technique for enhancing the bandwidth, the structure of a single intermediate cavity is replaced by pairs or triplets of artificially loaded cavities with Q factors dropped to half or one-third, respectively, of the cavity they replace. The individual cavities in each cluster should be positioned so that they are significantly isolated from one another. Also, the lossy ceramic materials are employed as absorbers to prevent any potential coupling between the subunits. At the University of Maryland, Nusinovich *et. al.* discussed the formalism related to the stagger tunned clustered-cavity gyro klystron and observed a significant enhancement in bandwidth in contrast to the conventional structure [172]. The performance improvement in clustered cavity gyro klystron, operated in Ka band, is reported in [80] has observed an increment in bandwidth from 0.34% to 1.2%, and also been a modest improvement in the gain and efficiency. Sinitsyn *et. al.* compared the clustered cavities against the multicavity gyro klystrons and concluded that the clustered approach had advantages in terms of bandwidth, gain, and gain bandwidth product, also observed that the positioning of the clustered portion is critical for maximum efficiency and gain [173].

The present chapter discusses:

- An approach to developing clustered cavity-based gyro-twystron amplifiers that maximize the bandwidth with the less compromise in gain and efficiency than traditional gyro-twystron designs.
- The complete design of the device as well as the beam wave interaction is discussed, using the commercially available CST particle studio.
- Also, the performance improvement of the clustered cavity-based gyro-twystron is validated and compared with the reported stagger tuned gyro -twystron.

5.2. Analysis and Design of Interaction Circuit

To simplify the calculation, some assumptions are used, i.e., neglecting the space charge effect and ignoring the beam effect on the field inside the cavity. The different cavities, as well as the clusters inside the cavities, are isolated enough from each other. To avoid crosstalk between the two cavities, an isolation factor of 40 dB is considered here. Taking into account all of the aforementioned assumptions, the gyrating motion of electrons in gyro amplifier is described by the generalized nonlinear equations as follows:

$$\frac{\partial(\gamma\beta_{\perp})}{\partial l} = \frac{(\gamma\beta_{\perp})^{s-1}}{\beta_{\parallel}} \mathrm{Re}\left\{F_{g,h} f(l) e^{is\phi}\right\} \qquad [5.1]$$

$$\frac{\partial(\phi)}{\partial l} = \frac{(\gamma c k_0 - s\Omega_0)}{s\gamma c\beta_{\parallel}} + \frac{(\gamma\beta_{\perp})^{s-1}}{\gamma\beta_{\perp}\beta_{\parallel}} \mathrm{Img}\left\{F_{g,h} f(l) e^{is\phi}\right\} \qquad [5.2]$$

Where $\beta_{\perp}$ and $\beta_{\parallel}$ are the transverse and axial velocity divided by the speed of the light related to the electron momentum. ϕ, l, γ, k_0 and s are the electron gyro phase, axial length, relativistic factor, wave number in a vacuum and the harmonic number, respectively. F is a normalized field in the h cavity of the g cluster and is defined as,

$F = \frac{eA}{cm_0\Omega_0\gamma_0}\left(\frac{s}{2}\right)^{s-1}\frac{\beta_{\perp 0}^{s-4}F_L}{(s-1)}$, where A is the field amplitude, Ω_0 is the cyclotron frequency, and F_L is the Lorentz force. $f(l)$ is the axial structure of the normalized field. In multi-cavity based gyro amplifiers, the cavity designed to follow the point gap model. The electron momentum at the entrance of the any cavity of the cluster is defined as $p\left(l_{g,h}=0\right)=1+\sum_{g<g',h<h'}\mathrm{Re}\left\{F_{g',h'}e^{i\phi_{d,g'-1}}\right\}$, here $\phi_{d,g'-1}$ is electron gyrating phase at the end of the p-1cluster and depends on the phase and momentum at the entrance, frequency mismatching (∇) and section length. Similarly, the electron phase at the entrance of the cavity is calculated as $\phi\left(l_{g,h}=0\right)=\phi_0+\sum_{g'<g}\left[\nabla-p_{g'}^2\left(L_{g'}\right)\right]L_{d,g'}+\sum_{h'<h}\mathrm{Re}\left\{iF_{g,h'}e^{i\phi_{d,g-1}}\right\}$ is depends on the length of the previous section, cumulative bunching of the gyrating beams and the electron momentum. The RF wave amplification is susceptible to the beam wave interaction and this susceptibility is calculate as $\chi_{g,h}=-i-\frac{2i}{F_{g,h}}\sum_{h'<h}F_{g,h'}-\frac{2i\left\langle e^{-i\phi_{d,g-1}}\right\rangle}{F_{g,h}}$ and describe the dependency of susceptibility on the electron bunching, the number of the cavity, and the gyrating phase. This susceptibility leads to the field development in the input cavity being defined as:

$$F_{g,h}\left\{1+i\delta_{g,h}+iI_{0(g,h)}\chi_{g,h}\right\}+A_h=0 \qquad [5.3]$$

where A_h is complex field amplitude in the h^{th} cavity and $\delta_{g,h}$ is the frequency detuning between operating frequency and cavity resonating frequency of h cavity of g cluster, I_0 are the normalized current, depending on the cavity's Q factor and the beam current. The developed field intensity and phase in different clusters are defined as

$$\left|F_{g,h}\right|^2 = \frac{4I_{0(g,h)}^2 \left|\overline{F}_{g,h}\right|^2}{\left(1+I_{0(g,h)}\right)^2 + \delta_{g,h}^2} \qquad [5.4]$$

$$\tan\left(\phi_{sig} - \chi_{g,h}\right) = \frac{\delta_{g,h}F_{g,h}^{'} - F_{g,h}^{''}\left(1+I_{0(g,h)}\right)}{\delta_{g,h}F_{g,h}^{''} + F_{g,h}^{'}\left(1+I_{0(g,h)}\right)} \qquad [5.5]$$

Where $F_{g,h}^{'}$ and $F_{g,h}^{''}$ are the real and imaginary part of the function $\overline{F} = e^{-i\phi_{sig}}\left(\sum_{h^{'}<h} F_{g,h^{'}} + \left\langle e^{-i\phi_{d,g-1}}\right\rangle\right)$, depends on the RF signal amplitude and phase, field intensity and phase inside the cavity.

The developed electric field at the output cluster depends on the susceptibility and phase as:

$$\left|F_{2,2}\right| e^{i\left(\theta_{2,2}\text{-}f_{sig}\right)} = \frac{\left(1\text{-}I_{0(2,1)} + i\delta_{2,1}\right)\left(\text{-}2J_1(\Phi)I_{0(2,2)}\right)}{\left(1+I_{0(2,1)} + i\delta_{2,1}\right)\left(1+I_{0(2,2)} + i\delta_{2,2}\right)} \qquad [5.6]$$

where Φ is the bunching parameter directly related to the drift tube length and the field in the previous cavity and used to define the gyrating phase at the cluster entrance.

In the beam wave interaction process, the gyrating electron transfers its orbital energy to the RF wave; that energy is defined the orbital efficiency. The orbital efficiency is varies with the bunching parameters, different phase value and the position of the cluster cavity, is defined as: $\eta_{\perp} = \sum_{g,h}\left|F_{g,h}\right|^2 \chi_{g,h}^{''}$ where $\chi_{g,h}^{''}$ is the complex term of the susceptibility. For the multi cavity clustered based structures, the orbital efficiency is

$$\eta_{\perp} = 2J_{1(\Phi\Sigma)}\sum_{h<N}\left|F_{g,h}\right|\cos\phi_{g,h} - \sum_{h<N}\left|F_{g,h}\right|^2 - 2\sum_{h<N}\sum_{h^{'}<h}\left|F_{g,h}\right|\left|F_{g,h^{'}}\right| \qquad [5.7]$$

here the *N* is the number of cavity and $\phi_{g,h}$ is the signal phase inside the *h* cavity of the *g* cluster.

The ballistically bunched gyrating beam in the drift tube section will encounter the entrance of the interaction region and build a field that is reliant on the beam's susceptibility in the following ways:

$$\left|F_{g,h}\right| e^{i\left(\phi_{g,h}-\phi_{sig}\right)} = \frac{\left(1-I_{0(g,h-1)}+i\delta_{g,h-1}\right)\left(-2J_h\left\{\Phi\right\}I_{0(g,h)}\right)}{\left(1+I_{0(g,h)}+i\delta_{g,h}\right)\left(1+I_{0(g,h-1)}+i\delta_{g,h-1}\right)} \quad [5.8]$$

The overall gain of the stagger tuned cluster cavity-based gyro-twystron is the superposition of constant gain and variable gain, and express as: $G_T = G_{const} + G_{\text{var}}$, where G_{const} is the gain of the synchronously tuned gyro-twystron, and G_{var} is the variable gain and defined as the function of bunching parameter, electrons gyrating phase, cluster position and frequency detuning and the corresponding expression is

$$G_{\text{var}} = 10\log\left[1+\left\{\left(\delta_{g,h-1}+\delta_{g,h}\right)^2/4\right\}\right] - 10\log\left[\left(1+\delta_f^2\right)\left(1+\delta_{g,h-1}^2\right)\left(1+\delta_{g,h}^2\right)\left(1+\delta_l^2\right)\right] \quad [5.9]$$

Here δ_f and δ_l are frequency detuning between operating frequency and the resonating frequency of first and last cavity, respectively.

The nonlinear analysis discussed above is carried out to examine the output performance of the clustered-cavity gyro-twystron amplifier shown in Fig 5.1. The operating point of the current clustered cavity gyro-twystron is depends on the interaction region of the beam mode line and operating TE_{01} mode line in dispersion diagram, shown in Fig 5.2. It is observed from the dispersion characteristic that the operational mode and the beam mode line interact with one another in a positive wave number direction. This results in convective instability and initiates the process of amplification. A computer friendly numerical code is written to analyze the beam-wave interaction mechanism in the clustered-cavity gyro-twystron. This code provides a comprehensive solution to the present designed clustered-cavity gyro-twystron and solved for the bandwidth and gain variation. The electrical and mechanical parameter

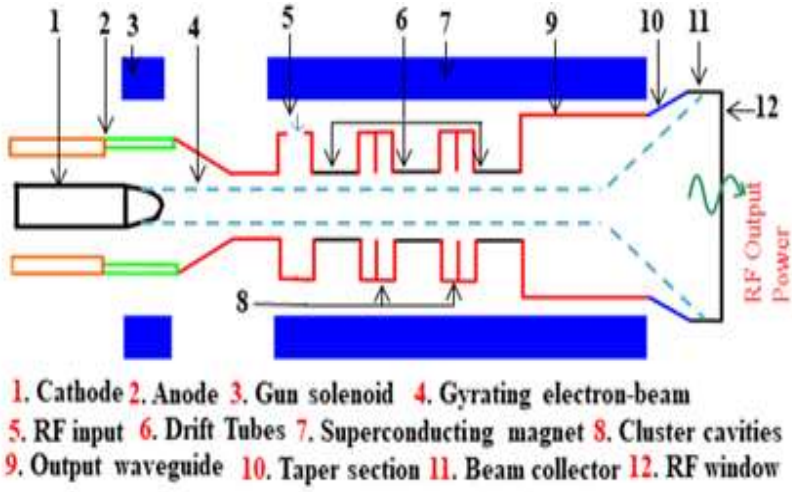

Figure 5. 1. Schematic of cluster cavity gyro-twystron.

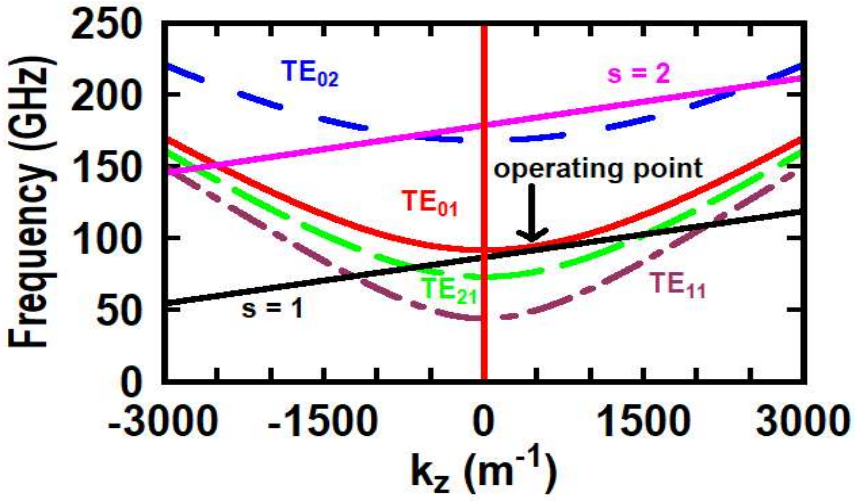

Figure 5. 2. Dispersion diagram of W-band clustered cavity gyro-twystron.

shown in Table. I is used for design and analysis purpose. As in clustered cavity technique quality factor played a crucial role in bandwidth enhancement, so the quality factor of each cavity in the first cluster is optimized as $Q_{1,1} = 56$ and $Q_{1,2} = 56$, similarly for the second cluster $Q_{2,1} = 51$ and $Q_{2,2} = 51$. Figure 5.3 and Fig 5.4 shows the bandwidth and gain variation, respectively as a function of stagger tuning parameter corresponding to the stagger tuned clustered cavity gyro-twystron and conventional gyro-twystron (stagger tuned conventional cavity gyro-twystron).

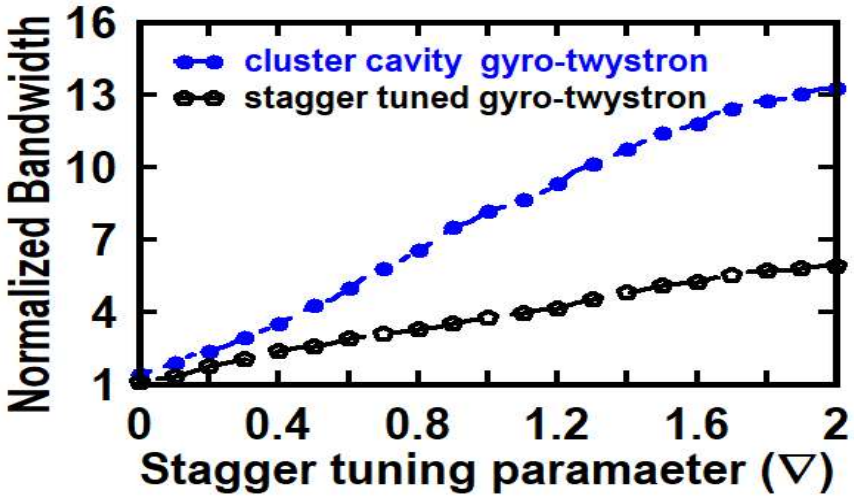

Figure 5. 3. Normalized bandwidth variation of clustered cavity gyro-twystron and stagger tuned gyro-twystron as a function of stagger tuning parameter.

A staggered tuned cavity effectively increases the bandwidth as tuning is increased but also leads to a drop in gain. It is shown in Figure 5.3, the bandwidth of the clustered cavity method is twice. that of the stagger tuning method for a stagger tuning value of 0.6, and this is because the quality factor of clustered cavity has been kept half as compared to the quality factor of stagger tuned cavity. Stagger tuning and clustered cavity are the two different techniques to enhance the bandwidth. Still, due to the difference in the used cavity design, the clustered cavity approach developed superior bandwidth compared to the stagger tuning approach, while the gain decrement is

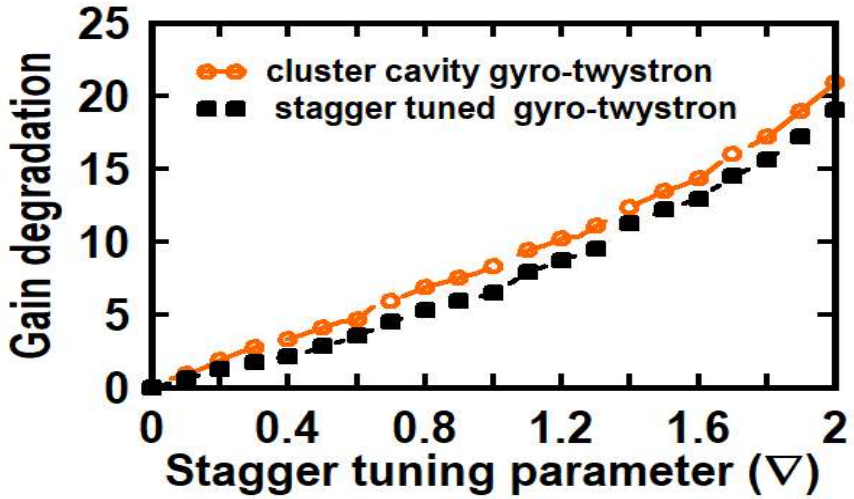

Figure 5. 4. Gain decrement in clusterd cavity gyro-twystron and stagger tuned gyro-twystron as a function of stagger tuning parameter.

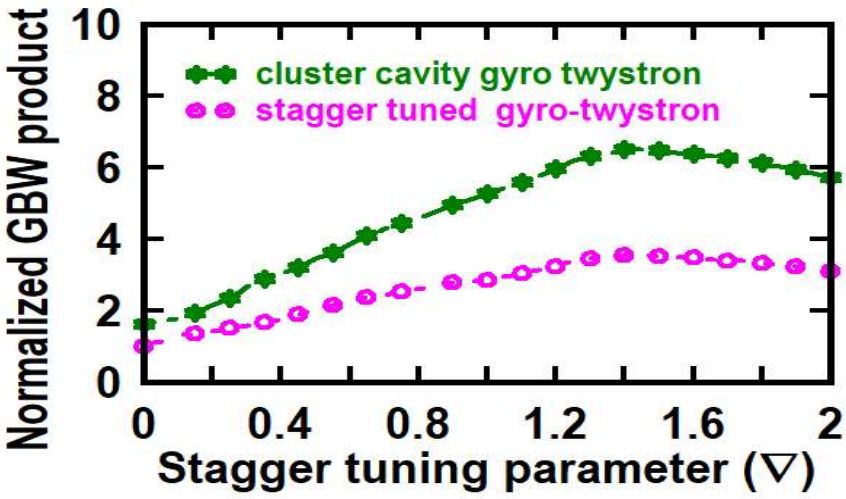

Figure 5. 5. Change in normalized gain bandwidth product in clustered cavity gyro-twystron and stagger-tuned gyro-twystron as a function of stagger tuning parameter.

almost the same in both methods (Figure5.4). The higher enhancement in bandwidth and lesser decrement in gain leads an effective gain bandwidth product for clustered cavity gyro-twystron, make it suitable for various radar applications. The variation in normalized gain- bandwidth product as a function of stagger tuning parameter is shown in Figure5.5. It is noted that after a certain value of stagger tuning, the typical normalized gain-bandwidth product experiences some decrement, which is owing to a substantial reduction in gain after a certain value of stagger tuning. While using the same stagger tuning parameter, the clustered cavity approach greatly increases the normalized gain-bandwidth product due to effective bandwidth advancement and lesser losses in gain.

5.3. Modeling and Cold Simulation

To validate the analytical finding of the clustered cavity approach, the complete gyro-twystron structure is modelled and simulate in 3-D code CST Particle Studio [134], based on finite integration technique (FIT). The electrical and mechanical parameters given in Table 5.1 is used to design the wide band clustered cavity gyro-

twystron, shown in Figure 5.6. The structure, modelled in CST environment with appropriate boundary conditions, follow the hexahedral messing, a volume discretization technique. This messing converts the complete design into miniature form and computer accessible format. To maintain the acceptable tradeoff in between accuracy and simulation time, the complete structure is meshed with 10 cells per wavelength. This selection of meshing automatically generates the total mesh cells of

Table 5. 1. DESIGN PARAMETERS OF CLUSTERED CAVITY GYRO-TWYSTRON

RF subsection		**Length (mm)**	**Radius (mm)**	**Particulars**	**Values**
Input Cavity		7	1.989	Beam Voltage	65 kV
Clustered Cavities	I	7.8	1.989	Beam Current	6 A
	II	8.2	1.989	Magnetic Field	3.66 T
Drift Tube I, II, III		11	1.45	Velocity spread	4 %
Waveguide		12	1.989	Velocity ratio	1.6

4192812 with the smallest and largest cell size of 0.0422 and 0.3045, respectively. The different cavities and drift tubes are modelled separately and observed the developed field, operating mode, frequency, using the cold (beam absent) simulation. The extent of the cavities is determined by the operating frequency and mode. The designed cavity is optimized for monitoring the susceptibility of the electron beam to the RF wave, resulting in effective beam modulation. The radius $r_c = x_{mn}c/\omega_c$ of the cavity is determined by the operating mode's eigenvalue (x_{mn}) and the cut-off frequency (f_c). The cut-off frequency (f_c) of TE_{mnd} is defined as $f_c = \left(c/2\pi\sqrt{\mu_r\varepsilon_r}\right)\left(\sqrt{\left(x_{mn}/r_c\right)^2+\left(\pi d/l_c\right)^2}\right)$, where μ_r, ε_r, d and l_c are the relative permittivity, relative permeability, half wave periodicity in axial direction and cavity length.

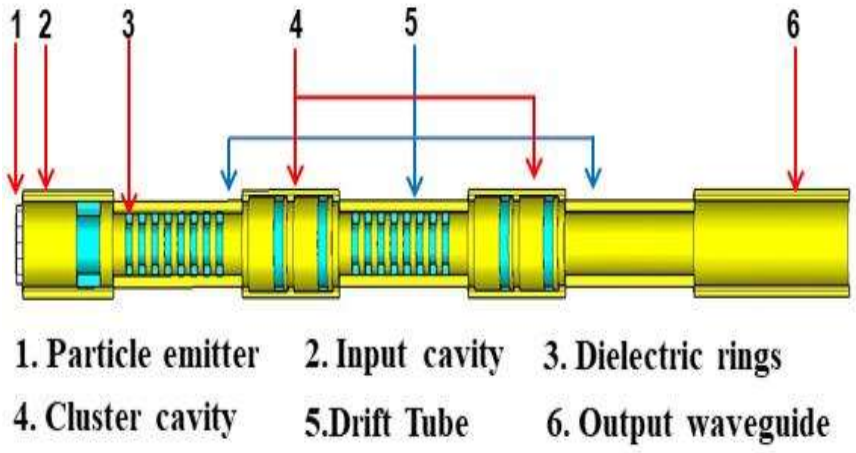

Figure 5. 6. CST model of clustered cavity gyro-twystron.

For the stable operation and optimize the quality factor, the cavities are loaded with the dielectric material Beryllium Oxide-Silicon Carbide (BeO- SiC), having the dielectric constant of $\varepsilon_r = 11.52 - j3.55$ and loss tangent of 0.308. The Eigen mode solver is used to compute the resonating frequency and operating mode of the cavity.

To avoid the field leakage in adjacent sections, a field free drift tube is placed between them, that provide sufficient isolation in between the adjacent cavities and waveguide. The dimensions of the drift tube are optimized as to provide the effective isolation as well as avoid the beam interception with the drift tube wall. The drift tube radius (r_{dt}) is depends on the following inequalities $r_{dt} < x_{mn}c/2\pi f$ and $r_b < r_{dt} < r_c, r_w$, where r_b and r_w are the gyrating beam radius and waveguide radius. The length (L_{dt}) of the drift tube section is depends on the isolation required in between the adjacent section and the ballistic beam bunching occurrence inside the drift tube. As the overall efficiency of the amplifier is depends on the how efficiently the bunched electron transfer its energy to the RF wave and the this transformation is depends on the bunched electrons energy, therefore the length of the drift tube is kept enough to provide the sufficient beam bunching and effective isolation between the various cavities and in

between the cavity and waveguide. The drift tube length is computed as: $L_{dt} = 5.75 \Big/ \sqrt{\left(x_{mn}/r_{dt}\right)^2 - \left(\omega/c\right)^2}$, where ω is the device operating frequency.

The bunched electron beams transfer its energy to the RF wave in the waveguide interaction region. The axial length of the interaction section is optimized as to provide the efficient amplification as well as avoid the oscillation. The waveguide length (L_w) is kept below the start oscillation length, depends on the current and defined as: $L_w = \dfrac{15.82\left(x_{mn}^2 - m^2\right) J_m^2 \beta_{\|}^2 k_{\|} \gamma_o I_A}{4\beta_{\perp}^2 k_{\perp}^4 I_b \left(J_{m\pm s}\left(k_{\perp} r_g\right)\right)^2 \left(J_n^{'}\left(k_{\perp} r_l\right)\right)^2}$, where I_A is the Alfven current and r_g, r_l are the electron beam guiding center radius and Larmor radius, respectively.

5.4. PIC Simulation Results

The energized gyrating electron beams, bunched in the drift section enter into the interaction region and interact with the RF wave. This beam wave interaction mechanism is studies using the 3D particle in cell (PIC) solver of the commercially available CST particle studio. In CST particle studio the predefined emission models are available for generating the gyrating electron beams. A circular perfect electric conducting (PEC) particle source with the kinetic parameters is selected for the gyrating electron beam generation. The generation of the beams depends on the beam voltage and current that varies the beam energy, velocity and momentum. The shape of the gyrating beam depends on their guiding radius and Larmor radius and selected as it avoids the interception with the wall and spread in velocity. The beam voltage of 65 kV is converted into the velocity as a kinetic type using the Lorentz factor (γ) and pitch factor of 1.6 as in tangent form. The electron beams generating with the beam current of 6 A are having the outer radius and inner radius of ~ 0.7149 mm and ~1.1126 mm

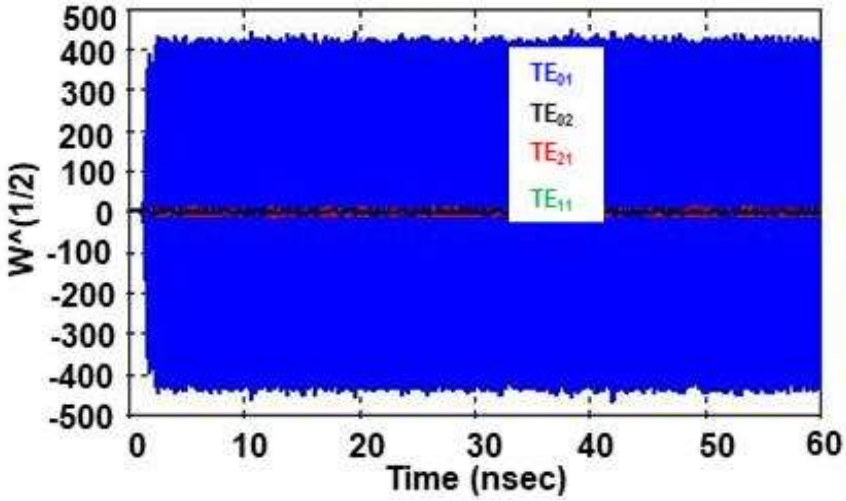

Figure 5. 7. Temporal growth of E-field in operating TE_{01} mode and other competing modes.

respectively, depends on the guiding radius of ~ 0.9135 mm and Larmor radius of ~ 0.1991 mm. This gyrating beam enters into the input cavity and get modulated after interacting with the applied RF input and attain the ballistic bunching in the field free drift tube section. The energized beams interact with the electromagnetic waves in the output waveguide section. The beam wave interaction is taken place under the guidance of the constant magnetic field of ~ 3.66 T, that control the synchronism between gyrating beam and electromagnetic wave. In this beam wave interaction, the RF wave get amplified after extracting the kinetic energy of the transverse moving electron of the gyrating beams. To receive an amplified RF wave an output port is defined at the end of the structure and performed postprocessing to obtain the output power. The applied input signal at the input port developed an electric field in operating TE_{01} mode, at the output port as shown in Figure5.7 with the maximum amplitude of ~ 400 keV. This developed electric field is used in post processing feature available in CST particle studio to compute the generated RF output power. The temporal growth of the output signal yielded an instantaneous power of ~160 kW with the time average value of ~ 82 kW, corresponding to the 20 W input signal (Figure 5.8). The electronic efficiency and saturated gain of the clustered cavity-based amplifier is ~ 21 % and ~36 dB,

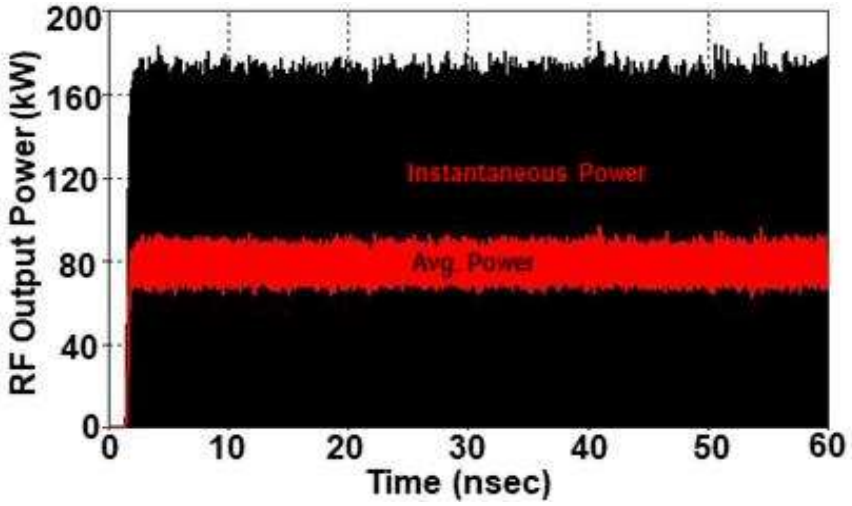

Figure 5. 8. Temporal growth of the output power signal developed in operating in TE_{01} mode.

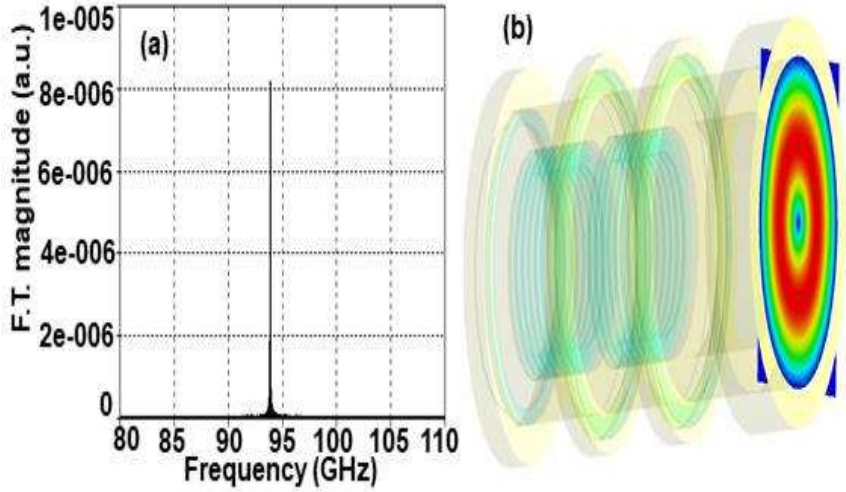

Figure 5. 9. Frequency spectrum of the operating TE_{01} mode developed at output port, (b) contour plot of the operating TE_{01} at the output port.

corresponding to the beam voltage of 65 kV and beam current of 6 A. Figure5.9 show the operating frequency and the operating mode of the output signal, computed at the output port using the post processing and ensure that the present gyro-twystron is operating in fundamental TE_{01} mode at 94 GHz.

5.5. Parametric Analysis and Validation

The various electrical parameters, such as magnetic field, beam voltage, beam current, velocity ratio, and velocity spread, have been tuned in order to achieve the goal of the

amplifier's performance. This will make it possible for the output power, efficiency, bandwidth, and gain to be increased to their maximum levels. Figure5.10 shows the variation in output power with the frequency, corresponding to the different velocity spread. The power amplification in the interaction region is dependent on the synchronization of beam waves, which in turn is dependent on the spread in velocity of the gyrating beam. The Figure 5.10 shows a drop in output power as the speed increases because the synchronization is disrupted and the for the present design ~ 82 kW power is obtained for the 4 % velocity spread. The beam wave synchronism is controlled by the cyclotron frequency, and this cyclotron frequency varies with the magnetic field. The applied DC magnetic field also force the electron beam to remain in confined and any variation in magnetic field causes a shift in beam orientation. This variation in beam movement induced a shift in beam wave synchronism, which result in a change in device output power, as observed in Figure 5.11. The RF power conversion depends on the effect of the magnetic field on the change in frequency and the maximum power and bandwidth at the magnetic field of 3.66 T. As a relativistic device, the gyro- twystron's performance is also relative to the applied voltage. Any change in applied voltage causes a change in the relativistic factor gamma, which disrupts beam wave

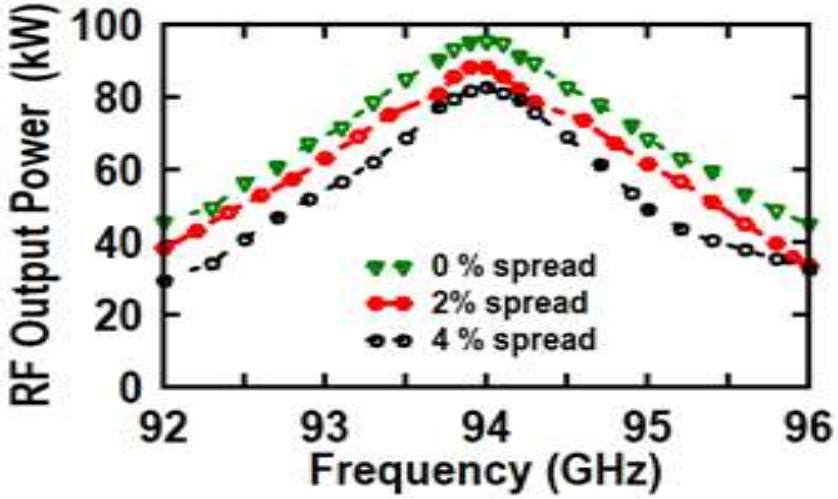

Figure 5. 10. Output power variation with the frequency corresponding to the different velocity spread.

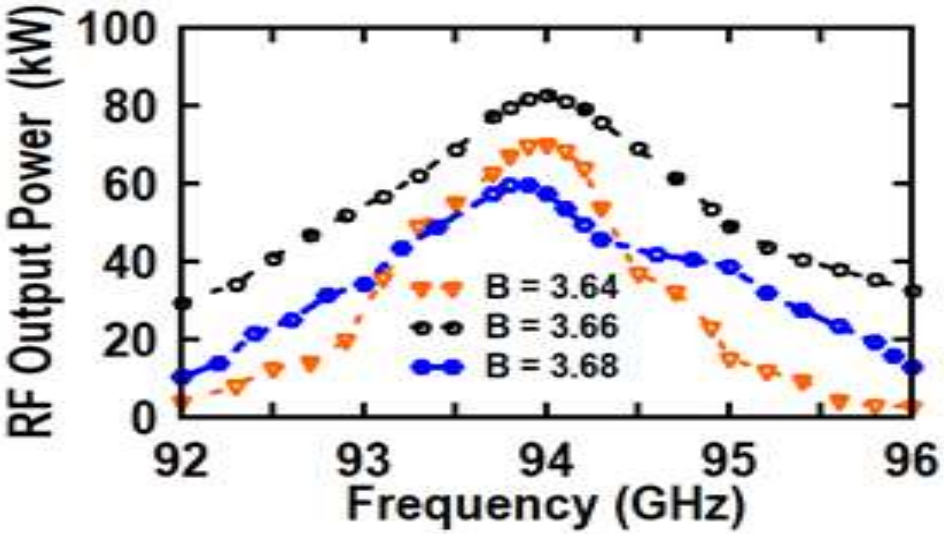

Figure 5. 11.Output power variation with the frequency corresponding to the different magnetic field.

synchronism and the amplifier's output. From Figure 12 (a) the maximum RF output is observed at 65 kV and degradation in output is found at voltage above and below the operating voltage of 65 kV. The movement of the gyrating electron beam is controlled by the applied dc voltage, that alters the velocity ratio and spread in the electron velocity ratio or the pitch factor that is a crucial parameter of gyrating electron beam. The variation in output power corresponding to velocity ratio is shown in Figure12 (b) and observed an increment in power with the velocity ratio. However, beyond the

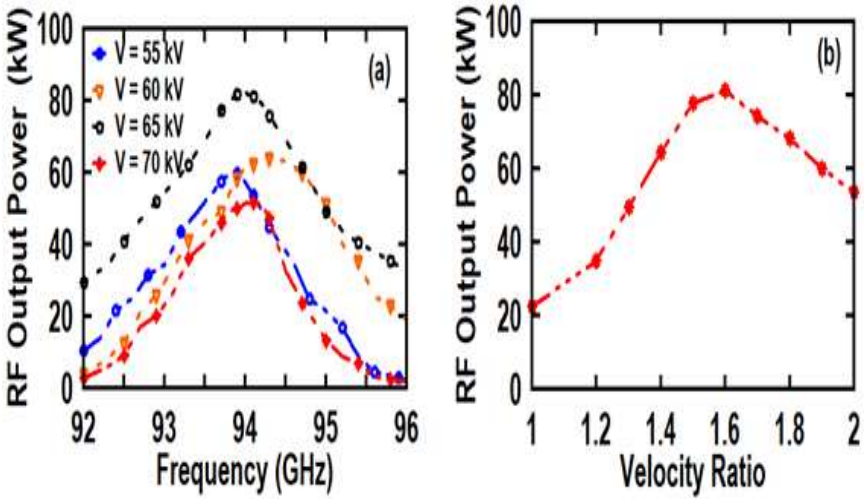

Figure 5. 12. (a) Output power variation with the frequency corresponding to the applied beam voltage, (b) change in output power with the velocity ratio.

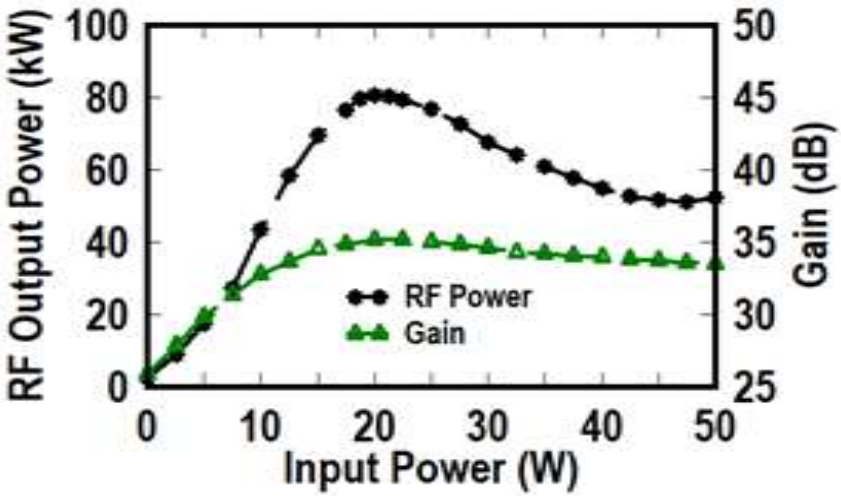

Figure 5. 13. Output power growth and gain corresponding to the RF input power.

desired value of velocity ratio (1.6) the output power decreases because the higher value of velocity ratio shifts the beam current and interaction length toward the SOC and SOL that degrade the device performance. The change in output power and gain with respect to the drive input power is shown in Figure 5.13 and observe a maximum power at the drive input of 20 W and beyond this value, the power and gain begin to decreases due to the occurrence of the neighboring cyclotron harmonics in the RF output power. The analytical finding of the clustered cavity gyro-twystron is validated with the 3-D PIC simulation (Figure 5.14)

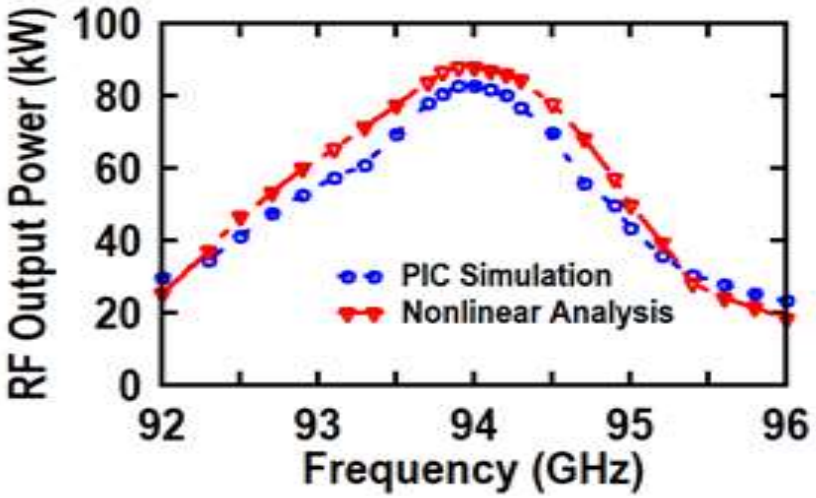

Figure 5. 14. Validation of analytical result with the PIC simulation output.

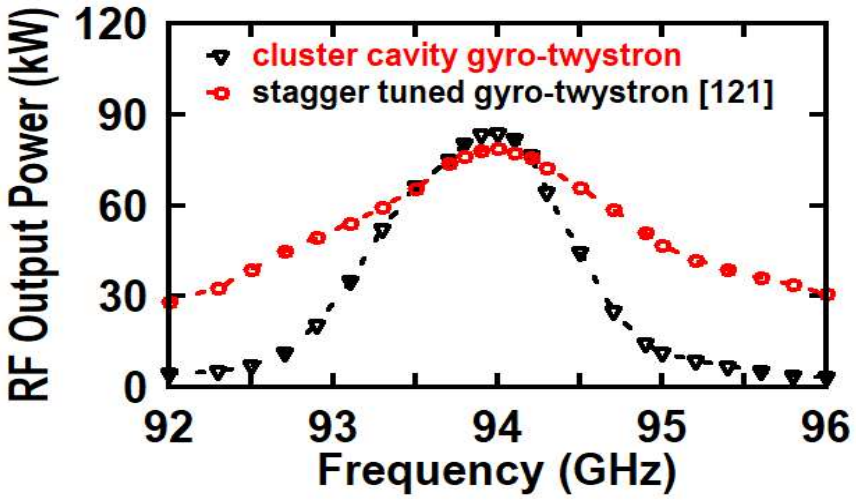

Figure 5. 15. Performance comparison of the clustered cavity gyro-twystron and stagger tuned gyro-twystron.

agreement The PIC simulation of the present clustered cavity gyro-twystron predicted the RF output power ~ 82 kW in operating TE_{01} mode against the analytical finding of ~ 85 kW as shown in Figure 5.14. The advantage of the clustered cavity gyro-twystron over the stagger tuned gyro-twystron presented in [121] is shown in Figure 5.15 and observed an effective improvement in bandwidth (~3 GHz) compared to the stagger tuned bandwidth of 1.4 GHz with the acceptable degradation in RF out power.

5.6. Conclusion

In this chapter a clustered cavity approach is adopted to widen the bandwidth of the W-band gyro-twystron with the minimum compromise in gain or efficiency. The analytical theory related to the clustered cavity based gyro-amplifiers is used to optimized the gyro-twystron performance and validated through commercially available simulation tool, “CST Particle Studio”. The clustered cavity gyro-twystron is modelled and simulated in 3-D PIC simulation tool, “CST Particle Studio” to observe the beam wave interaction behaviour and its outputs. The findings of the PIC simulation of the present cluster cavity approach are:

- The RF output power of ~ 82 kW at 94 GHz in operating TE_{01} mode with a gain of ~ 36 dB for the RF input of 20 W. The electronic efficiency of the present gyro-twystron is ~ 21 % corresponding to the beam voltage and current of 65 kV and 6 A, respectively.
- The bandwidth of the present clustered cavity gyro-twystron is ~ 3 GHz, which is twice as large as the bandwidth (~1.4 GHz) reported in stagger tuned gyro-twystron [121].
- This effective enhancement in bandwidth with the very least decrement in gain produces a large gain bandwidth product, making the present W-band clustered cavity gyro-twystron an important source for various radar applications.